ORIGINAL RESEARCH

Check for updates

Validation of radiolabelled exendin for beta cell imaging by ex vivo autoradiography and immunohistochemistry of human pancreas

Theodorus J.P. Jansen[1], Sevilay Tokgöz[1], Mijke Buitinga[2,3], Sanne A.M. van Lith[1], Lieke Joosten[1], Cathelijne Frielink[1], Esther M. M. Smeets[1], Martijn W.J. Stommel[4], Marion B. van der Kolk[4], Bastiaan E. de Galan[5,6,7], Maarten Brom[1], Marti Boss[1] and Martin Gotthardt[1]*

Abstract

Background Estimation of beta cell mass is currently restricted to evaluating pancreatic tissue samples, which provides limited information. A non-invasive imaging technique that reliably quantifies beta cell mass enables monitoring of changes of beta cell mass during the progression of diabetes mellitus and may contribute to monitoring of therapy effectiveness. We assessed the specificity of radiolabelled exendin for beta cell mass quantification in humans. Fourteen adults with pancreas tumours were injected with ^{111}In-labeled exendin-4 prior to pancreatic resection. In resected pancreas tissue, endocrine-exocrine ratios of tracer uptake were determined by digital autoradiography and accumulation of ^{111}In-labeled exendin-4 was compared to insulin and GLP-1 receptor staining. Of four participants, abdominal single photon emission computed tomography/computed tomography (SPECT/CT) images were acquired to quantify pancreatic uptake in vivo

Results Tracer uptake was predominantly present in the endocrine pancreas (endocrine-exocrine ratio: 3.6 [2.8–10.8]. Tracer accumulation showed overlap with insulin-positive regions, which overlapped with GLP-1 receptor positive areas. SPECT imaging showed pancreatic uptake of radiolabelled exendin in three participants.

Conclusion Radiolabelled exendin specifically accumulates in the islets of Langerhans in human pancreas tissue. The clear overlap between regions positive for insulin and the GLP-1 receptor substantiate the beta cell specificity of the tracer. Radiolabelled exendin is therefore a valuable imaging agent for human beta cell mass quantification and has the potential to be used for a range of applications, including improvement of diabetes treatment by assessment of the effects of current and novel diabetes therapies on the beta cell mass.

Trial registration ClinicalTrials.gov NCT03889496, registered 26,032,019, URL https://clinicaltrials.gov/study/NCT03889496?term=NCT03889496. ClinicalTrials.gov NCT04733508, registered 02022021, URL https://clinicaltrials.gov/study/NCT04733508.

*Correspondence:
Martin Gotthardt
Martin.Gotthardt@radboudumc.nl

Full list of author information is available at the end of the article

Introduction

A reliable technique to non-invasively image and quantify beta cell mass would have great potential to contribute to a better understanding of the changes in beta cell mass during the progression of diabetes mellitus. Other potential applications include assessment of the effects of novel therapies (e.g. aimed at preserving or restoring beta cell mass or beta cell replacement therapies) and aiding in the selection of the most suitable treatment option. Such applications require a technique that enables accurate quantification of small changes in beta cell mass over time.

Until now, beta cell mass has mostly been studied by immunohistochemical analysis of human pancreas tissue. The availability of human samples is however limited, since biopsies of the pancreas have a high risk for complications and are thus discouraged in individuals who are otherwise healthy, whether with or without diabetes [1]. Current knowledge on beta cell mass is therefore limited to data from human samples after autopsy or pancreatectomy (thus reflecting a single time point mostly in a late phase of the disease), or estimations based on the beta cell function rather than mass (e.g. stimulated C-peptide levels). In addition, the determination of beta cell mass based on immunohistochemical analysis of tissue is prone to sampling errors, since analysis of the complete pancreatic tissue specimen is laborious and time-consuming so that usually only certain regions of the pancreas are selected.

An attractive approach to non-invasively image beta cell mass is the use of nuclear imaging techniques with tracers specifically targeting the beta cells. Such tracers should have high affinity for a beta cell specific target, resulting in high uptake in beta cells with low background uptake (i.e. in other endocrine cells and the exocrine pancreas), for its successful application for quantification of beta cell mass. Several tracers targeting different receptors have been developed for this purpose and currently exendin-based tracers seem to be the best-suited candidates [2–4]. The stable glucagon-like peptide 1 (GLP-1) analogue exendin specifically targets the GLP-1 receptor, highly expressed by beta cells [5].

We have previously shown that pancreatic uptake of radiolabelled exendin strongly correlates with the beta cell mass and not alpha cell mass [6, 7] and is not influenced by insulitis [3, 4]. We have also demonstrated significantly lower pancreatic uptake of radiolabelled exendin-4 in humans with type 1 diabetes compared to healthy subjects [6] and a correlation of beta cell mass with glycaemic control [8]. In addition, we have demonstrated a significant amount of pancreatic tracer uptake in some individuals with longstanding type 1 diabetes [8], data in line with studies showing that people with type 1 diabetes may have more remaining beta cell mass (up to >50%) than was previously thought [9–12]. Furthermore, intrahepatically transplanted islets of Langerhans could be detected in humans with radiolabelled exendin [13]. These findings underline the great potential of GLP-1 receptor positron emission tomography (PET) imaging for (longitudinal) in vivo determination of beta cell mass in humans.

As a final validation step, we aim to provide data demonstrating the specificity of exendin uptake in the islets of Langerhans in the human pancreas. For this purpose, we injected individuals scheduled for pancreas resection with $[^{111}\text{In}]\text{In-Lys}_{40}(\text{Ahx-DTPA})]$exendin-4 prior to surgery and assessed the pancreatic uptake of the tracer through ex vivo autoradiography of the obtained human pancreatic samples and single photon emission computed tomography/computed tomography (SPECT/CT).

Materials and methods

Study participants

Study participants were recruited from the outpatient clinic at the Department of Surgery in the Radboud university medical center (Nijmegen, the Netherlands). All individuals had a minimum age of 18 years and were scheduled for (partial) pancreatic resection after being diagnosed with a pancreatic tumour (see Table 1). One of these individuals had dexamethasone-induced diabetes, others did not have diabetes. Recent blood samples that were taken for standard laboratory tests prior to surgery were used to assess kidney function and liver enzymes. All study procedures were performed in the Radboud university medical center. Participants were included from two clinical studies with similar inclusion and exclusion criteria (Clinicaltrials.gov ID NCT03889496 and NCT04733508). Although intended for more study participants, funding for the trial was terminated early as a consequence of the COVID 19 pandemic (NCT03889496). Another challenge was the inclusion of participants since we frequently encountered unexpected changes in surgery date affecting the planning of the study or changes in treatment plan resulting in no surgery at all (instead, most patients were included in clinical studies receiving chemotherapy), which have led to early termination of NCT04733508. Notwithstanding these unforeseen situations, the data acquired from both studies with the current number of inclusions are sufficient to answer our research question.

Table 1 Clinical characteristics

Patient	Age	Sex	BMI	Type of surgery	Diagnosis	Diabetes
1	73	Male	27.8	Pancreaticoduodenectomy	Ductal adenocarcinoma	No
2	58	Male	25.3	Tail resection	Insulinoma	No
3*	66	Female	25.9	Pancreaticoduodenectomy	Ductal adenocarcinoma	Yes**
4	70	Male	29.6	Corpus-tail resection with splenectomy	Neuroendocrine tumour and gastral branch-duct intraductal papillary mucinous neoplasm	No
5	74	Female	21.7	Pancreaticoduodenectomy	Mixed-duct intraductal papillary mucinous neoplasm	No
6*	45	Female	22.0	Pancreaticoduodenectomy	Intestinal type adenocarcinoma	No
7*	77	Male	27.5	Tail resection	Side-duct intraductal papillary mucinous neoplasm	No
8*	65	Male	22.0	Corpus-tail resection with splenectomy	Pancreas carcinoma	No
9*	67	Male	35.1	Pancreaticoduodenectomy	Intraductal papillary mucinous neoplasm	No
10*	50	Female	23.1	Corpus-tail resection with splenectomy	Pancreas carcinoma	No
11*	37	Female	21.9	Tail resection	Multilocular mucinous cyst in pancreas corpus	No
12*	40	Male	33.5	Tail resection	Neuroendocrine tumour in pancreas tail	No
13*	52	Female	27.8	Pancreaticoduodenectomy	Pancreas carcinoma	No
14*	50	Male	21.1	Pancreaticoduodenectomy	Pancreas carcinoma	No

*No SPECT/CT scan **Dexamethasone-induced diabetes (since the year 2000)

Preparation and labelling of ^{111}In-labeled exendin-4

Preparation and labelling of $[^{111}\text{In}]$In-[Lys$_{40}$(Ahx-DTPA)] exendin-4 (where Ahx represents aminohexanoic acid) for clinical use was produced (piCHEM, Graz, Austria), dissolved and portioned according to GMP standards to a final concentration of 2 µg/ml in 1 mol/L HEPES (pH 5.5) containing 0.1% Tween-80. The vials were stored at −20 ℃. Radiolabelling was performed by adding exendin-DTPA to the vial containing $[^{111}\text{In}]$InCl$_3$ (Curium, Petten, the Netherlands) to a final concentration of 150 MBq ^{111}InCl$_3$ per µg [Lys$_{40}$(Ahx-DTPA)]exendin-4 (molar activity of 72 GBq/µmol). After incubation at room temperature for 20 min 0.150 mL EDTA (3.75 mg/ ml) was added. Due to regulation changes during the runtime of the project, additional purification steps were added to the procedure to remove the excess of HEPES. Therefore, the labelling procedure for the final patient included subsequent purification of $[^{111}\text{In}]$In-[Lys$_{40}$(Ahx-DTPA)]exendin-4 on an HLB cartridge (Waters, UK) and by gel filtration on a PD-10 column. The end product was sterilized by passing through a 0.2 µm filter (Millex GV) in a Hotcell Class A. Quality control was performed by reversed-phase high performance liquid chromatography (RP-HPLC) and instant thin layer chromatography (ITLC). Labelling efficiency was determined on Varian silicagel strips (ITLC-SG, Agilent Technologies, Amstelveen, the Netherlands) using 0.1 mM ammonium acetate buffer with 0.1 mM EDTA, pH 5.5 as the mobile phase. RP-HPLC was done using a C18 reversed-phase column (HiChrom alltima C18, Breda, the Netherlands). For elution, a linear gradient of 0.1% TFA in acetonitrile (3–100% over 10 min with a flow rate of 1 ml/min) was used. The labelling efficiency was 99.9% and the purification with HLB and PD-10 was necessary for the reduction of HEPES concentration.

Administration of ^{111}In-exendin and image acquisition

After a 4-hour fasting period, participants received an intravenous injection with 151±5 MBq $[^{111}\text{In}]$In-Lys$_{40}$(Ahx-DTPA)]exendin-4 (further referred to as ^{111}In-exendin) (peptide dose of ∼1 µg) as a slow bolus over 1 min. In the first seven participants, SPECT/CT images of the abdomen were acquired on a Siemens Symbia T16 SPECT/CT system, using the low-dose CT (without contrast) for anatomical correlation (total scanning time of approximately 45 min). For the SPECT acquisition, 128 views were obtained with an acquisition time of 40s per view. The acquired SPECT/CT images were reconstructed as previously described [6]. The other participants underwent surgery and the resected pancreatic tissue was used for microSPECT/CT imaging (MILabs, Utrecht, The Netherlands). A 1 h microSPECT/CT scan of the resected pancreatic tissue was performed using a 1.5-mm diameter pinhole rat collimator tube followed by a CT scan for anatomical reference. The microSPECT/CT was reconstructed according to the following parameters: 0.8 voxel size, 4 iterations and 128 subsets using pixel-based similarity-regulated ordered subsets expectation maximization (SROSEM) algorithm. A gaussian filter of 2.5 mm was applied to the microSPECT images.

Quantification of SPECT/CT images

Reconstructed SPECT/CT images were analysed using Inveon Research Workplace 4.1 software (Siemens Healthcare). Three spherical volumes of interest (VOIs) of 9.6 mm were manually placed in the pancreatic head, corpus, and between head and corpus. Positions for each VOI were localized on the CT scan. To determine the pancreatic uptake of ^{111}In-exendin, the counts measured in the VOIs were corrected for the administered activity (MBq), the time after injection (t_{scan}-$t_{injection}$), and the half-life of indium-111 ($t_{1/2}$=2.81 days).

Jansen *et al. EJNMMI Research* (2024) 14:96

Page 4 of 9

$$Exendin\ uptake = \frac{Counts}{Administered\ activity \times \left(\frac{1}{2}\right)^{\frac{(t_{scan}-t_{injection})}{t_{\frac{1}{2}}}}} \quad (1)$$

Autoradiography and immunohistochemistry of pancreatic tissue

Surgical resection of pancreatic tissue was done one day after injection of the radiotracer. On the day of surgery, frozen sections of 4 μm were obtained from the resected pancreatic tissue and fixated with ice cold acetone for 10 min before autoradiography. The dried sections were exposed to a phosphor imager screen (Fuji Film BAS-SR 2025; super resolution) for a period of 2 weeks.

The slides used for autoradiography (frozen tissue sections) were incubated with a guinea pig-anti-insulin antibody (1:750 in phosphate buffered saline (PBS)+1% bovine serum albumin (BSA) ab195956, Abcam, Cambridge, UK) for 60 min at room temperature (RT) in a humidified chamber. Slides were then washed 3 times with 10 mM PBS and incubated with goat-anti-guinea pig-HRP (1:1000 in PBS+1% BSA, A18775 Thermo Fisher) for 30 min at RT. After washing 3 times with 10 mM PBS, the bound antibodies were visualized using diaminobenzene (DAB, Bright DAB, BS04 Immunologic, VWR, Dublin, Ireland). Slides were counterstained for 5 s with hematoxylin (Klinipath, Olen, Belgium). Tissue was mounted with a cover slip using Permount (Fisher Scientific, Waltam, MA, USA).

Formalin fixed and paraffin embedded pancreas tissue was sectioned at 4 μm thickness. Sections were deparaffinized with xylene and rehydrated in ethanol. Antigen retrieval was performed with TRIS- buffered EDTA (TBE)+0,05% Tween-20 in a PT Module (Thermo Fisher Scientific, Waltam, MA, USA) (10 min at 96 °C). Slides were washed 3 times with tris buffered saline (TBS)+0.05% Tween-20 between all the incubation steps. Endogenous peroxidase activity was quenched with 3% H_2O_2 for 10 min, followed by an incubation of 30 min at RT with 20% normal goat serum+0.1 M glycine in PBS in a humidified chamber. Sections were stained with Mouse-anti-GLP-1 receptor (1:10, DSHB Mab 3F52, Iowa City, IA, USA) for 2 h at RT. After washing, the slides were incubated with Bright Vision poly HRP-GAM/Rb IgG (Immunologic, VWR, Dublin, Ireland). The bound antibodies were visualized using diaminobenzene (DAB, Bright DAB, BS04 Immunologic, VWR, Dublin, Ireland). Slides were counterstained with hematoxylin (Klinipath, Olen, Belgium) and mounted with a cover slip using Permount (Fisher Scientific, Waltam, MA, USA).

Adjacent sections were stained for insulin and underwent antigen retrieval with 10 mM citrate pH 6.0 in a PT Module (Thermo Fisher Scientific, Waltam, MA, USA) (10 min at 96 °C). Slides were washed 3 times with 10 mM PBS between all the incubation steps. Endogenous peroxidase activity was quenched with 3% H_2O_2 for 10 min, followed by an incubation of 30 min at RT in 20% normal goat serum. The slices were incubated with guinea pig-anti-insulin (1:500, ab195956, Abcam, Cambridge, UK) for 60 min at RT. After washing, the slides were incubated with goat anti guinea pig-HRP (1:1000, A18775 Thermo Fisher) for 30 min at RT. The bound antibodies were visualized using diaminobenzene, counterstained and mounted as described before.

Image acquisition of tissue sections

Sections that were stained for insulin and the GLP-1 receptor were scanned with an automated microscope (Pannoramic 1000 (P1000)) using an objective magnification of 20x, resulting in pixel size of 0.24 μm (in x- and y-direction). The obtained digital images and the previously mentioned autoradiography images allowed to check for overlap between insulin-positive areas, GLP-1 receptor positive areas, and radiotracer uptake.

Endocrine-to-exocrine ratio

Ratios between endocrine and exocrine tissue were determined using the digital autoradiographic images analysed with MATLAB (R2018a; MathWorks, Natick, MA, USA). First, the complement of the autoradiographic image was computed so that high pixel values correspond with high uptake of ^{111}In-exendin in the image. The average pixel value of the background was determined by manually drawing a region of interest (ROI) in the image. Exocrine and endocrine tissue were excluded from the ROI to exclude signal from exendin uptake in the tissue. Subsequently, six ROIs were drawn in different locations in the exocrine tissue to acquire the average pixel value from these exocrine regions. These ROIs were drawn in regions with low fat content. In total, 10 ROIs were positioned in endocrine regions (Islets of Langerhans) to again obtain the average pixel value from these ROIs combined. Locations of all ROIs were carefully placed in the image and were always based on the section stained for insulin after it had been used for autoradiography, to localize the desired regions (background, exocrine or endocrine tissue; see Supplementary Fig. 1 for graphical representation of the analysis). To correct for the background activity, the average pixel value from the background ROI were subtracted from the exocrine and endocrine ROIs. This enabled to calculate the endocrine to exocrine ratio corrected for the background signal.

Statistical analysis

Data were expressed as mean±SD, median (interquartile range (IQR)), or number (%). Relationships between parameters were checked for linearity using the Pearson correlation coefficient (r), with a two-tailed analysis of variance. The level of significance was set at $p < 0.05$.
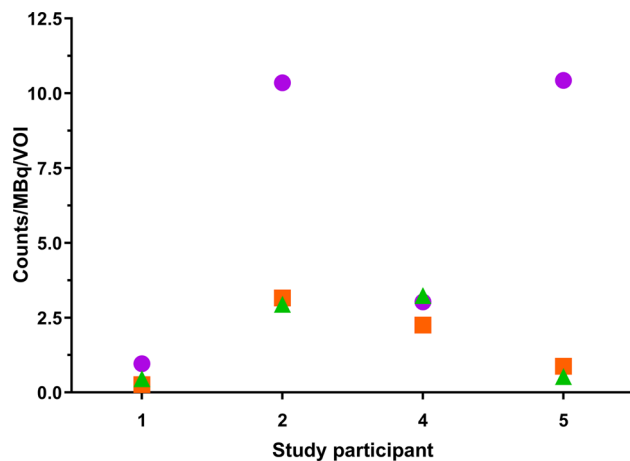
Jansen *et al. EJNMMI Research*   (2024) 14:96

Page 5 of 9

Fig. 1 Quantification of the pancreatic uptake of ^{111}In-labelled exendin Uptake of radiolabelled exendin in the pancreatic head (in purple), corpus (in green), and at a position between the head and corpus (in orange) were quantified in the SPECT/CT images of four imaged participants. Uptake in each volume of interest (VOI) was corrected for administered activity (MBq) and time after injection

GraphPad Prism software was used for all analyses (GraphPad Prism 10 for Windows, San Diego, California USA).

Results

Fourteen adults (6 women and 8 men) who were scheduled for pancreatic resection were included. The types of surgery and diagnosis differed among individuals (Table 1). No study-related adverse events were observed in any of the study participants.

Participants 3, 6 and 7 were injected with ^{111}In-exendin, but declined to undergo SPECT/CT (participating in study NCT03889496). Participants 8 to 14 (participating in study NCT04733508 in which pre-operative SPECT/CT was not part of the protocol) were also injected with ^{111}In-exendin, and after surgery their resected pancreatic tissue was used for ex vivo microSPECT/CT imaging. Quantification of the in vivo SPECT/CT images of the other four participants demonstrated highest uptake of exendin in the VOI of the pancreatic head (5.10±4.39 counts/MBq), and to a lesser extent in the VOI of the corpus (1.60±1.53 counts/MBq) and in the VOI placed between the head and corpus (1.48±1.34 counts/MBq). Uptake of ^{111}In-labeled exendin in the pancreata of the participants is shown in Fig. 1 and corresponding SPECT/CT images can be found in Fig. 2. In addition, clear uptake of ^{111}In-exendin was visible in the resected pancreatic tissue of participant 14 (Supplementary Fig. 2).

Comparison of the autoradiography and insulin staining demonstrated clear overlap between the accumulation of the tracer and the insulin-positive regions (Fig. 3), showing the specific uptake of the tracer in the islets of Langerhans. Comparison of the insulin and GLP-1 receptor staining on the pancreas tissue showed overlap of these markers (Fig. 4), demonstrating the specificity of the GLP-1 receptor as a target for beta cells.

The mean endocrine-exocrine ratio of the tracer uptake, determined by analysis of the digital autoradiography images of all participants, was 3.6 [2.8–10.8] (Fig. 5). The median endocrine-exocrine ratio of the
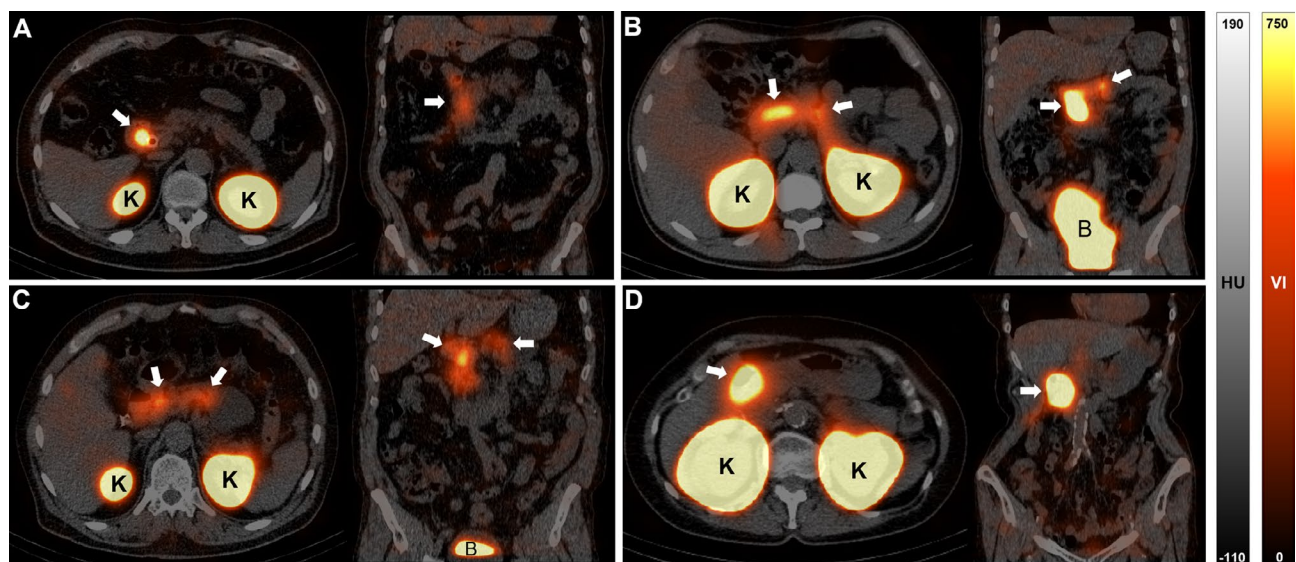

Fig. 2 Abdominal SPECT/CT images showing uptake of ^{111}In-exendin Images acquired through SPECT/CT imaging showing uptake of exendin in the pancreas (white arrows) in participant 1 (**A**), 2 (**B**), 4 (**C**) and 5 (**D**). Highest uptake is seen in the kidneys on the transversal cross-section resulting from the renal clearance of exendin (indicated with 'K'). On the coronal cross-sections, activity present in the bladders of participant 2 and 4 is visible (indicated with 'B'). Hounsfield unit (HU). Voxel intensity (VI)
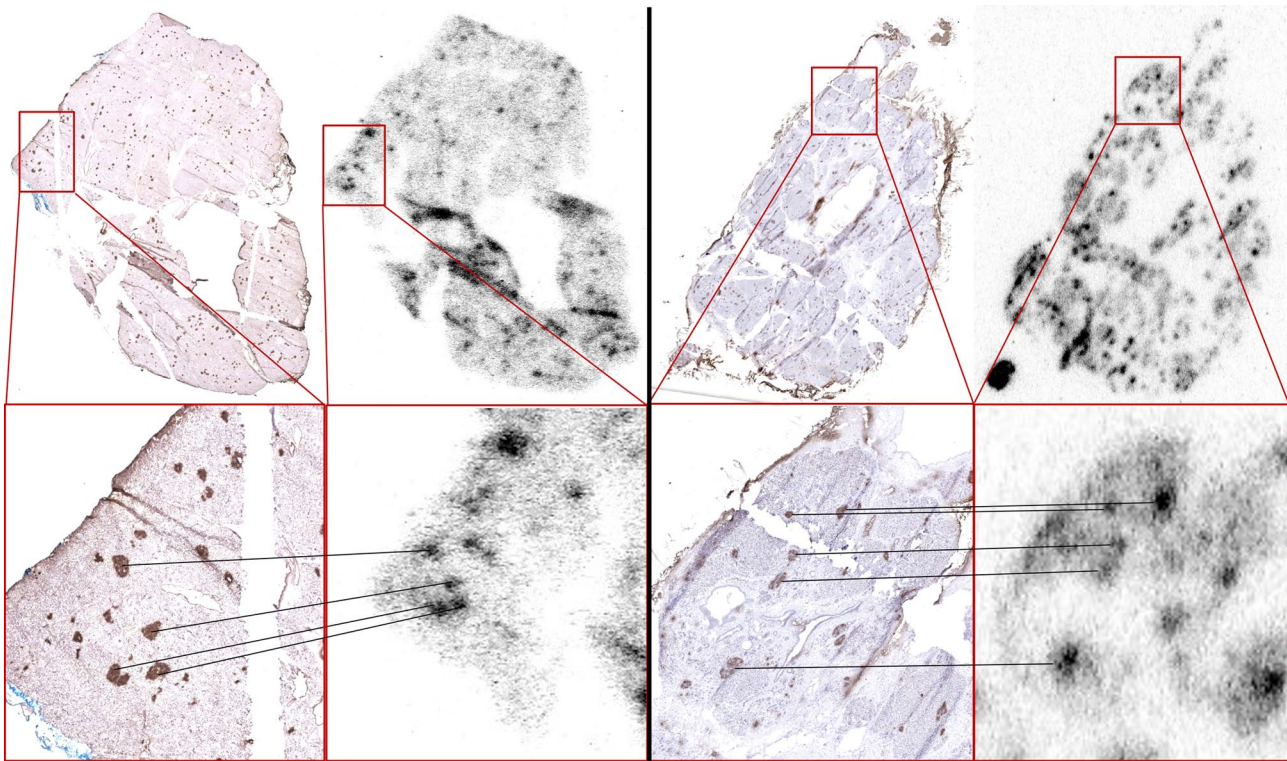
Fig. 3 Overlap between uptake of ^{111}In-exendin on autoradiographic images and insulin staining in pancreatic islets Ex vivo autoradiography and immunohistochemistry on frozen sections showing overlap of ^{111}In-exendin accumulation and insulin-positive regions in human tissue – proofs localization of the tracer to the islets (participant 2 (left) and participant 5 (right))

tracer uptake based on all slides was 3.1 [2.6–8.6] (Supplementary Fig. 3). The endocrine-exocrine ratio of participant 1 was excluded from the analysis because of insufficient image quality for reliable quantification (red star in Fig. 5 and Supplementary Fig. 3).

Discussion
In this study, we obtained human validation data for the use of radiolabelled exendin as a tracer for beta cell imaging confirming previously obtained animal data [3, 4, 6, 7]. Our findings demonstrate that ^{111}In-labeled exendin accumulates specifically in the endocrine pancreas, with high uptake values compared to the exocrine pancreas. The specificity for the endocrine pancreas is substantiated by the overlap of the tracer uptake with insulin-positive areas. Using immunohistochemical staining we also show the specific expression of the GLP-1 receptor in insulin-positive areas, confirming its adequacy as a target for beta cells.

These data demonstrate that radiolabelled exendin is a reliable tracer for non-invasive beta cell imaging in humans. Several other radiotracers have been investigated for beta cell imaging. However, ^{11}C-labeled 5-hydroxytryptophan is a radiotracer for total endocrine pancreatic cell mass [14]. Dihydrotetrabenazine, targeting the vesicular monoamine transporter 2, is likely partially taken up in the exocrine pancreas and the target is not expressed in all beta cells while also being expressed in polypeptide cells [15, 16]. Quite recent data on the novel targets G protein-coupled receptor 44 [17–19] and the zinc transporter 8 [20] showed promising selective binding in beta cells, but further research is needed to substantiate the potential of these novel targets. Dopamine receptors expressed by beta cells [21] have also been explored as a possible target using the radioligand [11]C-(+)-4-propyl-9-hydroxynaphthoxazine (PHNO) [22]. This target seems to be solely expressed on functional, insulin-positive beta cells [22]. This in contrast to the GLP-1 receptor, which we showed to be expressed in beta cells of people with longstanding type 1 diabetes and undetectable C-peptide levels [23]. This would allow imaging of viable, dysfunctional beta cells. PHNO and exendin could thus both be useful or even be complementary techniques based on the research question.

Some limitations and aspects of this study need to be addressed. The small number of study participants was a limitation of this study. Inclusion was restricted to only individuals who were scheduled for pancreatic surgery, since taking biopsies from the pancreas for research purposes is unethical, limiting the availability of suitable candidates to be included in clinical studies [1]. A benefit of this study design is that it allowed us to assess the uptake
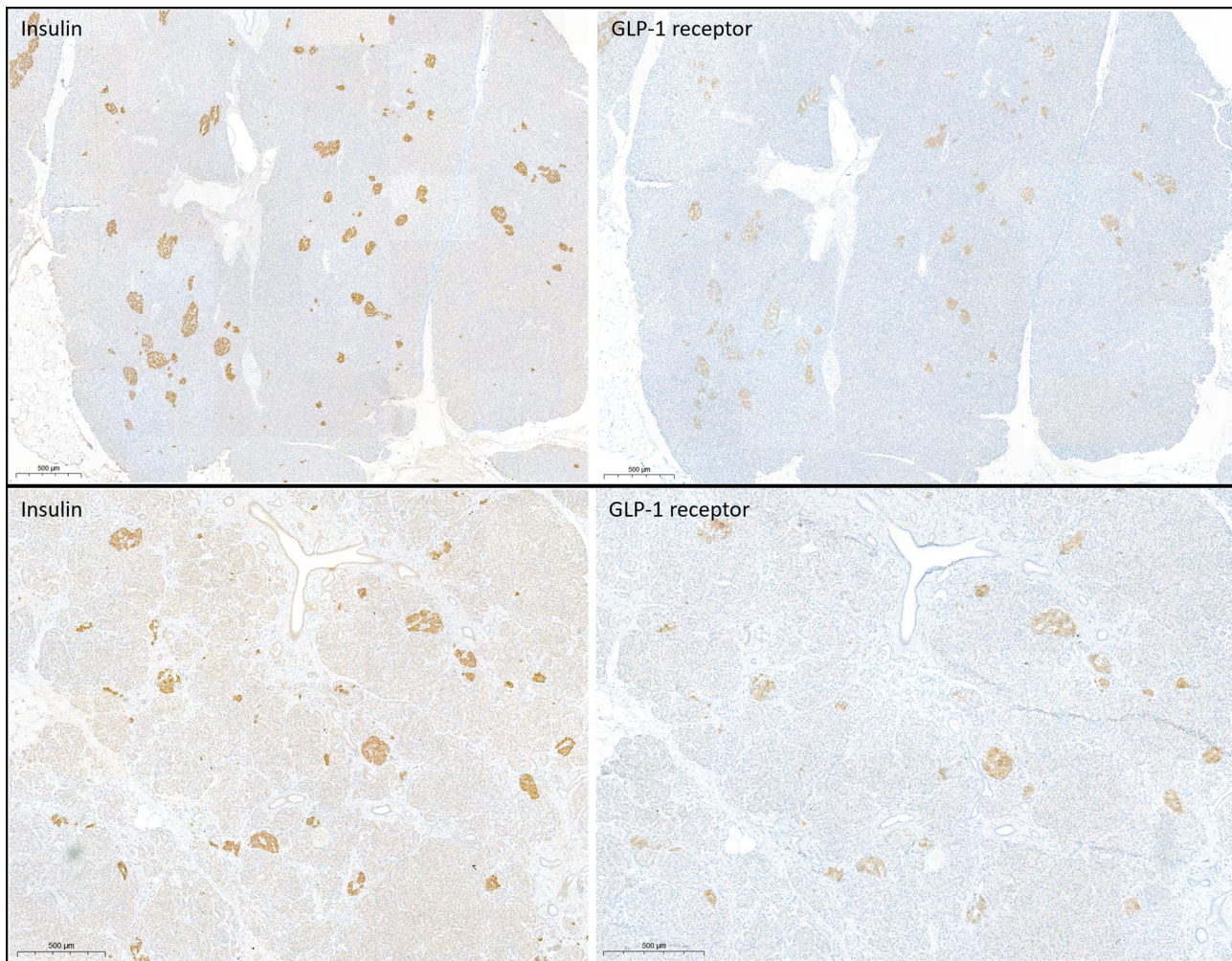
Fig. 4 Overlap between insulin staining and GLP-1 receptor expression in pancreatic islets Paraffin sections of pancreas tissue were stained for insulin and the GLP-1 receptor. The majority of GLP-1 receptor-positive areas show distinct overlap with insulin-positive areas in pancreatic islets

of the tracer in tissue shortly after injection. Patient inclusion was however complicated by the perceived burdensome nature of the study procedures (in particular the SPECT/CT scan scheduled one day before surgery), combined with the physical and mental effects of having suspected pancreatic cancer on the patients at the time of inclusion (see Table 1 for information on diagnosis). Another limitation is the amount of sections per participant, in some cases only one section could be included in the analysis, as a result of poor availability or quality of the tissue. Our recommendation is that in future studies even more effort should be made to include a higher number of sections per participant. In the current study we observed a 2 to 26-fold higher tracer uptake in the endocrine pancreas compared to the exocrine pancreas of the study participants, whereas significantly higher ratios up to 45 to 106-fold have been reported in rats [24]. GLP-1 receptor expression, measured by quantitative polymerase chain reaction (qPCR), is reportedly 47 times higher in the human endocrine pancreas than in the exocrine pancreas, while in rats they reported only 13 times higher expression in the endocrine pancreas [6]. The lower ratios we observed in this study most probably result from technical issues. The amount of radioactivity in the human tissue samples is very low compared to the amount in rats, leading to autoradiography images of much lower quality, resulting from the relatively much lower injected dose (150 MBq in humans vs. 15 MBq in rats, a 30-fold lower relative dose in humans) as well as the longer period between injection and acquisition of tissue samples (1-1.5 days for human samples vs. mostly 4 h for rodent samples). In addition to decay, the radionuclide had more time to wash out from the tissue for a longer period in humans.

In conclusion, this study revealed the specific accumulation of radiolabelled exendin in the islets of Langerhans in human pancreas tissue. Our findings validate the potential of radiolabelled exendin as a tracer for
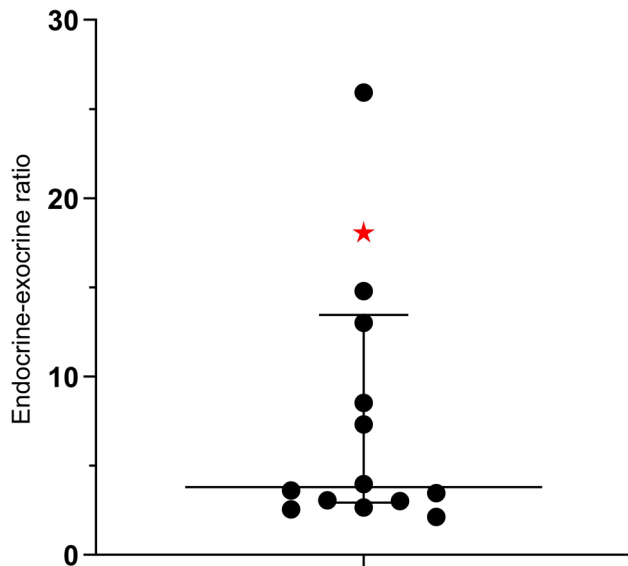
Fig. 5 Endocrine-exocrine ratio determined on digital autoradiography images Exocrine-endocrine ratio of the tracer uptake in pancreatic tissue samples of the study participants was 3.6 [2.8–10.8]. The ratio determined with the sample of participant 1 is excluded because of insufficient image quality for reliable quantification (red star in graph)

reliable non-invasive quantification of the beta cell mass in humans. Because of the low radiation dose of this technique, which we have shown before [25, 26], exendin imaging enables longitudinal assessment of beta cell mass within individuals to study changes over the course of diabetes progression or treatment effects over time.

Supplementary Information
The online version contains supplementary material available at https://doi.org/10.1186/s13550-024-01159-6.

Supplementary Material 1

Author contributions
LJ, MS, BG, MBr and MG designed the study. TJ, MBo, MBu, SL and ST performed the clinical study. MS and MK informed the patients and collected tissue samples. LJ and CF performed the immunohistochemistry. TJ, CF and ST performed the data analyses. All authors were involved in the interpretation of the results. TJ wrote the manuscript. All authors read and approved the final manuscript. MG is the guarantor of this work and, as such, had full access to all the data in the study and takes responsibility for the integrity of the data and the accuracy of the data analysis.

Data availability
The datasets used and/or analysed during the current study are available from the corresponding author on reasonable request.

Declarations

Consent to participate
Both clinical studies were approved by the local Ethics Committee (Commissie Mensgebonden Onderzoek regio Arnhem-Nijmegen, reference number NL47132.091.14 and NL63933.091.17). Both studies were performed in accordance with the ethical standards as laid down in the 1964 Declaration of Helsinki and its later amendments or comparable ethical standards. All study participants gave written informed consent.

Consent for publication
Written informed consent was obtained from the patients for publication of this study and accompanying images.

Competing interests
All other authors declare they have no conflicts of interest that are relevant to this study.

Author details
[1]Department of Medical Imaging, Radboud University Medical Center, Nijmegen, The Netherlands
[2]Nutrition and Movement Sciences, Maastricht University, Maastricht, The Netherlands
[3]Radiology and Nuclear Medicine, Maastricht UMC+, Maastricht, The Netherlands
[4]Department of Surgery, Radboud University Medical Center, Nijmegen, The Netherlands
[5]Internal Medicine, Radboud University Medical Center, Nijmegen, The Netherlands
[6]Internal Medicine, Maastricht UMC+, Maastricht, The Netherlands
[7]CARIM School for Cardiovascular Disease, Maastricht University, Maastricht, The Netherlands

References
1. Krogvold L, Edwin B, Buanes T, Ludvigsson J, Korsgren O, Hyoty H, et al. Pancreatic biopsy by minimal tail resection in live adult patients at the onset of type 1 diabetes: experiences from the DiViD study. Diabetologia. 2014;57:841–3. https://doi.org/10.1007/s00125-013-3155-y.
2. Eriksson O, Laughlin M, Brom M, Nuutila P, Roden M, Hwa A, et al. In vivo imaging of beta cells with radiotracers: state of the art, prospects and recommendations for development and use. Diabetologia. 2016;59:1340–9. https://doi.org/10.1007/s00125-016-3959-7.
3. Brom M, Joosten L, Frielink C, Peeters H, Bos D, van Zanten M, et al. Validation of (111)In-Exendin SPECT for the determination of the beta-cell Mass in BioBreeding Diabetes-Prone rats. Diabetes. 2018;67:2012–8. https://doi.org/10.2337/db17-1312.
4. Joosten L, Brom M, Peeters H, Bos D, Himpe E, Bouwens L, et al. Measuring the pancreatic beta cell Mass in Vivo with exendin SPECT during hyperglycemia and severe Insulitis. Mol Pharm. 2019;16:4024–30. https://doi.org/10.1021/acs.molpharmaceut.9b00728.
5. Tornehave D, Kristensen P, Romer J, Knudsen LB, Heller RS. Expression of the GLP-1 receptor in mouse, rat, and human pancreas. J Histochem Cytochem. 2008;56:841–51. https://doi.org/10.1369/jhc.2008.951319.
6. Brom M, Woliner-van der Weg W, Joosten L, Frielink C, Bouckenooghe T, Rijken P, et al. Non-invasive quantification of the beta cell mass by SPECT with (1)(1)(1)In-labelled exendin. Diabetologia. 2014;57:950–9. https://doi.org/10.1007/s00125-014-3166-3.
7. Brom M, Joosten L, Frielink C, Boerman O, Gotthardt M. (111)In-exendin uptake in the pancreas correlates with the beta-cell mass and not with the alpha-cell mass. Diabetes. 2015;64:1324–8. https://doi.org/10.2337/db14-1212.
8. Jansen TJP, Brom M, Boss M, Buitinga M, Tack CJ, van Meijel LA, et al. Importance of beta cell mass for glycaemic control in people with type 1 diabetes. Diabetologia. 2022;1–9. https://doi.org/10.1007/s00125-022-05830-2.
9. Oram RA, Sims EK, Evans-Molina C. Beta cells in type 1 diabetes: mass and function; sleeping or dead? Diabetologia. 2019;62:567–77. https://doi.org/10.1007/s00125-019-4822-4.

10. Yu MG, Keenan HA, Shah HS, Frodsham SG, Pober D, He Z, et al. Residual beta cell function and monogenic variants in long-duration type 1 diabetes patients. J Clin Invest. 2019;129:3252–63. https://doi.org/10.1172/JCI127397.
11. Keenan HA, Sun JK, Levine J, Doria A, Aiello LP, Eisenbarth G, et al. Residual insulin production and pancreatic ss-cell turnover after 50 years of diabetes: Joslin Medalist Study. Diabetes. 2010;59:2846–53. https://doi.org/10.2337/db10-0676.
12. Klinke DJ 2. Extent of beta cell destruction is important but insufficient to predict the onset of type 1 diabetes mellitus. PLoS ONE. 2008;3:e1374. https://doi.org/10.1371/journal.pone.0001374.
13. Jansen TJP, Buitinga M, Boss M, Nijhoff MF, Brom M, de Galan BE, et al. Monitoring beta cell survival after intrahepatic islet transplantation using dynamic exendin PET imaging: a proof-of-concept study in individuals with type 1 diabetes. Diabetes. 2023. https://doi.org/10.2337/db22-0884.
14. Ekholm R, Ericson LE, Lundquist I. Monoamines in the pancreatic islets of the mouse. Subcellular localization of 5-hydroxytryptamine by electron microscopic autoradiography. Diabetologia. 1971;7:339–48. https://doi.org/10.1007/BF01219468.
15. Schafer MK, Hartwig NR, Kalmbach N, Klietz M, Anlauf M, Eiden LE, Weihe E. Species-specific vesicular monoamine transporter 2 (VMAT2) expression in mammalian pancreatic beta cells: implications for optimising radioligand-based human beta cell mass (BCM) imaging in animal models. Diabetologia. 2013;56:1047–56. https://doi.org/10.1007/s00125-013-2847-7.
16. Saisho Y, Harris PE, Butler AE, Galasso R, Gurlo T, Rizza RA, Butler PC. Relationship between pancreatic vesicular monoamine transporter 2 (VMAT2) and insulin expression in human pancreas. J Mol Histol. 2008;39:543–51. https://doi.org/10.1007/s10735-008-9195-9.
17. Eriksson J, Roy T, Sawadjoon S, Bachmann K, Skold C, Larhed M, et al. Synthesis and preclinical evaluation of the CRTH2 antagonist [(11)C] MK-7246 as a novel PET tracer and potential surrogate marker for pancreatic beta-cell mass. Nucl Med Biol. 2019;71:1–10. https://doi.org/10.1016/j.nucmedbio.2019.04.002.
18. Eriksson O, Johnstrom P, Cselenyi Z, Jahan M, Selvaraju RK, Jensen-Waern M, et al. In vivo visualization of beta-cells by targeting of GPR44. Diabetes. 2018;67:182–92. https://doi.org/10.2337/db17-0764.
19. Jahan M, Johnstrom P, Selvaraju RK, Svedberg M, Winzell MS, Bernstrom J, et al. The development of a GPR44 targeting radioligand [(11)C]AZ12204657

for in vivo assessment of beta cell mass. EJNMMI Res. 2018;8:113. https://doi.org/10.1186/s13550-018-0465-6.
20. Eriksson O, Korsgren O, Selvaraju RK, Mollaret M, de Boysson Y, Chimienti F, Altai M. Pancreatic imaging using an antibody fragment targeting the zinc transporter type 8: a direct comparison with radio-iodinated Exendin-4. Acta Diabetol. 2018;55:49–57. https://doi.org/10.1007/s00592-017-1059-x.
21. Farino ZJ, Morgenstern TJ, Maffei A, Quick M, De Solis AJ, Wiriyasermkul P, et al. New roles for dopamine D2 and D3 receptors in pancreatic beta cell insulin secretion. Mol Psychiatry. 2020;25:2070–85. https://doi.org/10.1038/s41380-018-0344-6.
22. Bini J, Sanchez-Rangel E, Gallezot JD, Naganawa M, Nabulsi N, Lim K, et al. PET imaging of pancreatic dopamine D2 and D3 receptor density with (11)C-(+)-PHNO in type 1 diabetes. Journal of nuclear medicine: official publication. Soc Nuclear Med. 2020;61:570–6. https://doi.org/10.2967/jnumed.119.234013.
23. Boss M, Kusmartseva I, Woliner- van der Weg W, Joosten L, Brom M, Béhe M, et al. 111In-exendin spect imaging suggests presence of residual beta cells in patients with longstanding type 1 diabetes. Diabetologia. 2020;43(Abstract). https://doi.org/10.1007/s00125-020-05221-5.
24. Willekens SM, Joosten L, Boerman OC, Balhuizen A, Eizirik DL, Gotthardt M, Brom M. Strain Differences Determine the Suitability of Animal Models for noninvasive in vivo Beta cell Mass determination with radiolabeled exendin. Mol Imaging Biol. 2016;18:705–14. https://doi.org/10.1007/s11307-016-0936-y.
25. Boss M, Buitinga M, Jansen TJ, Brom M, Visser EP, Gotthardt M. PET-based dosimetry of [(68)Ga]Ga-NODAGA-exendin-4 in humans, a tracer for beta cell imaging. J Nuclear Medicine: Official Publication Soc Nuclear Med. 2019. https://doi.org/10.2967/jnumed.119.228627.
26. van der Kroon I, Woliner-van der Weg W, Brom M, Joosten L, Frielink C, Konijnenberg MW, et al. Whole organ and islet of Langerhans dosimetry for calculation of absorbed doses resulting from imaging with radiolabeled exendin. Sci Rep. 2017;7:39800. https://doi.org/10.1038/srep39800.

Publisher's note